Accepted Manuscript

Kalman filter-based ARAIM algorithm for integrity monitoring in urban environment

Hieu Trung Tran, Letizia Lo Presti

Please cite this article as: H.T. Tran, L.L. Presti, Kalman filter-based ARAIM algorithm for integrity monitoring in urban environment, *ICT Express* (2018), https://doi.org/10.1016/j.icte.2018.05.002

Kalman Filter-Based ARAIM Algorithm for Integrity Monitoring in Urban Environment

Hieu Trung Tran[1,*], Letizia Lo Presti[*]

Politecnico di Torino, Corso Duca degli Abruzzi 24, 10129 Turin, Italy

Abstract

This work proposes an adaptation of Advanced Receiver Autonomous Integrity Monitoring (ARAIM) algorithm for snapshot integrity monitoring in urban environment, using Kalman Filter (KF) as underlying positioning method. This new method can follow the changes of signal quality, maintaining good performance under the effect of multipath which is always presents in urban areas. Performance analysis using both simulated and real data validates the method, and comparison with conventional ARAIM algorithm (which was developed for aviation) further consolidates the suitability of the proposed method for urban scenario.

Keywords: ARAIM; integrity monitoring; Kalman filter; multipath; urban environment

1. Introduction

Integrity, as defined in [1], is the capability of a GNSS system to provide timely warning to users when the system becomes unreliable and should not be used for navigation purposes. In other words, integrity evaluates the level of trust a user can assign on the information provided by a system [2]. Integrity concerns the faults in navigation systems, such as satellites faults, incorrect ephemeris parameters, and any fault that could lead to hazardous outcome if the wrong information is used. Defined since the early days of GPS, the concept of integrity was designed for civil aviation use [2, 3]. Integrity has always been an important aspect of the navigation system, since the validity of navigation data could affect lives of many people.

A typical approach in aviation for integrity monitoring is called Aircraft-based Augmentation System (ABAS), which relies solely on the navigation data available on-board. This approach is implemented by the Receiver Autonomous Integrity Monitoring (RAIM) algorithms [4]. Recent works in navigation integrity [5, 6, 7, 8] for aviation have led to the next generation of RAIM algorithm, called Advanced RAIM (ARAIM) [5, 9], based on the solution separation (SS) approach. ARAIM improves the traditional RAIM in various ways, such as multi-constellation capability (traditional RAIM was developed solely for GPS), and generalized satellite fault hypothesis instead of single-fault hypothesis. ARAIM aims at providing better availability and lower Protection Level (PL) [10, 11, 12], making it suitable for more stringent phases of flight [9].

Although the concept of integrity was defined initially for civil aviation, it has gained interests in other applications as well, especially in those that require high reliability of the navigation data, such as Intelligent Transport Systems (ITS) and

Safety-of-Life (SoL) applications [13, 14]. It is important to note that, besides the accuracy of the positioning results as the most obvious criterion to evaluate the performance of a navigation system, integrity and continuity are also important performance parameters. The urban environment is very different from the aviation context, especially the limited number of visible satellites and the presence of multipath, both due to the reflection over buildings and structures. Multipath effect induces pseudorange errors and attenuation of receiving signal [15, 16], leading to higher positioning error.

Among numerous works on integrity monitoring in urban context, [18, 19] propose methods to evaluate PL using Satellite-based Augmentation System (SBAS), and as a result inherits the coverage issue of SBAS [2]. The studies of [3, 20], on the other hand, adapt the traditional RAIM method to urban context. However, the single-fault assumption of traditional RAIM is no more realistic and suitable for road traffic context [21, 22]. The authors of [23] proposed an adaptive RAIM method, based on Chi-square RAIM for urban canyon scenario. However, the work assumed all pseudorange measurement to have the same error variance, which is not suitable for such environment. The study in [24] discussed necessary changes when adapting ARAIM algorithm to urban context.

On the other hand, the work in [25] adapts the conventional ARAIM algorithm [9], which was developed on Least square (LS) positioning method, to Kalman Filter (KF). This paper will further improves [25], adapting this work into an SS ARAIM method based on KF for urban environment. The proposed method combines the advantages of the underlying techniques: the smoothness and high accuracy of KF, the good integrity performance and flexibility of SS ARAIM approach, and is suitable for urban scenario. The paper is organized as follows. Section 2 briefly introduces the KF-based ARAIM and discuss the choice of noise model for the adaptation. Section 3 presents implementation results on simulated and real data. Section 5 concludes the paper.

---

*Corresponding author

Email address: hieu.tran@polito.it (Hieu Trung Tran)

[1]Permanent address: NAVIS Centre, Room 602 Ta Quang Buu Library Building, Hanoi University of Science and Technology, No. 1 Dai Co Viet, Hanoi, Vietnam
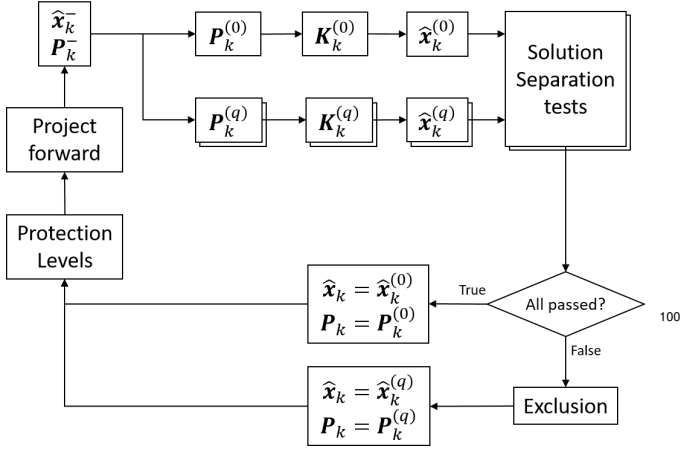
Figure 1: Scheme of the KF ARAIM algorithm for urban scenario

2. KF-based snapshot ARAIM for urban environment

The generic version of the KF-based snapshot ARAIM has been described in details in [25], along with the underlying KF model. As a result, this paper will retain similar notations for KF model as well as ARAIM algorithm for KF. The KF model utilizes a state vector $\boldsymbol{x}_k$ defined as:

$$\boldsymbol{x}_k = \begin{bmatrix} \boldsymbol{u}_k \\ -c\Delta t_{GPS,k} \\ -c\Delta t_{Gal,k} \\ \dot{\boldsymbol{u}}_k \\ -c\dot{\Delta}t \end{bmatrix} \tag{1}$$

where $\boldsymbol{u}_k \in \mathbb{R}^3$ is the position coordinate vector; Δt_{GPS} and Δt_{Gal} is the difference between the receiver's clock and system time of GPS and Galileo, respectively; c is the speed of light; $\dot{\Delta}t$ is the clock drift.

Conceptually, instead of predicting forward using the state transition matrix, the algorithm calculates the *fault-tolerant* Kalman gains $\boldsymbol{K}_k^{(q)}$, state corrections $\boldsymbol{x}_k^{(q)}$ and the error covariance matrices $\boldsymbol{P}_k^{(q)}$, using subsets of satellites (Figure 1). Each subset of satellites is called a *fault mode*, and can be considered a hypothesis of potential fault. Afterward, the initial all-in-view state vector $\boldsymbol{x}_k^{(0)}$ and fault-tolerant state vectors $\boldsymbol{x}_k^{(q)}$ are used as inputs for the Solution Separation tests, which measure the consistency of the measurement based on the deviation between these states. Should any test fails, the algorithm will attempt exclusion to find a consistent set of satellite, before proceeding to calculate the PL. The last step of each loop is to project the state vector and error covariance matrix ahead.

2.1. Choice of noise model

As pointed out in [24] and [25], one of the main changes when adapting ARAIM to urban environment is the noise model. An ideal noise model for urban scenario should be able to cover the multipath effect, which occurs due to presence of buidlings, trees and other obstacles. The original ARAIM algorithm uses a model called Airborne Accuracy Designator - Model A (AAD-A) [26, 27] which includes both random noise and MP error.

Parameters	Lightly degraded	Heavily degraded
a (m^2)	10	500
b $(m^2 Hz)$	150^2	10^6
$\dot{a}$ (m^2/s^2)	0.01	0.001
$\dot{b}$ $(m^2 Hz/s^2)$	25	40

Table 1: Example values for measurement error variance model

However, AAD-A was developed for airport environment [27], which is vastly different from urban environment. It is also worth mentioning that, while AAD-A evaluates multipath error based on elevation angle, the author of [28] observes a stronger correlation between pseudorange error (in urban context) and carrier-to-noise (C/N_0) ratio than elevation angle. As a result, an error model for urban use was proposed in [28] and has been chosen in this work. The measurement error covariance matrix $\boldsymbol{R}_k \in \mathbb{R}^{2N_{sat} \times 2N_{sat}}$ can be defined as:

$$\boldsymbol{R}_k = \begin{bmatrix} \boldsymbol{\Sigma}_k & \boldsymbol{0} \\ \boldsymbol{0} & \dot{\boldsymbol{\Sigma}}_k \end{bmatrix} \tag{2}$$

in which $\boldsymbol{\Sigma} \in \mathbb{R}^{N_{sat} \times N_{sat}}$ is a diagonal matrix, whose diagonal elements are the pseudorange error variances, while $\dot{\boldsymbol{\Sigma}}$ is a diagonal matrix containing the variances related to derivatives of pseudoranges. The diagonal elements of $\boldsymbol{\Sigma}$ and $\dot{\boldsymbol{\Sigma}}$ are defined as:

$$\boldsymbol{\Sigma}_{i,i} = a + b \cdot 10^{\frac{-C/N_{0,i}}{10}} \tag{3a}$$

$$\dot{\boldsymbol{\Sigma}}_{i,i} = \dot{a} + \dot{b} \cdot 10^{\frac{-C/N_{0,i}}{10}} \tag{3b}$$

where $C/N_{0,i}$ is the carrier-to-noise ratio of the signal from the i-th satellite which is time dependent, a, b, $\dot{a}$ and $\dot{b}$ are coefficients whose values depend on the assumed environment. Some examples of these coefficients are reported in Table 1 [28].

With this choice of noise model, the signal quality can affect on the PL. In case of multipath, the C/N_0 ratios of affected satellites drop, and this increases $\boldsymbol{R}_k$. As a result, separation variance $\sigma_s^{(q)}$ and detection threshold $T_{k,s}(q)$ (ARAIM parameters introduced in [25]) also increase for all fault mode. Note that $T_{k,s}(q)$ is calculated from $\boldsymbol{P}_{\Delta\hat{x}_k}^{(q)}$ which in turn is calculated using $\boldsymbol{R}_k$, hence the increase. Consequently, this leads to the general increase of PL, compared to less contaminated case. This argument will be later observed and confirmed in an experiment in Section 3.

3. Performance analysis

3.1. Simulation scheme

The adopted signal simulator is an updated version of [29], adding Galileo constellation and a multipath generator for urban environment. The multipath model being used is the Land Mobile Multipath Channel Model (LMMCM) [30] (which has been standardized in ITU document [31]), developed by the German Aerospace Center (DLR - Deutsche Zentrum für Luft- und Raumfahrt) using real data collected from numerous survey campaigns to investigate the effect of multipath in urban
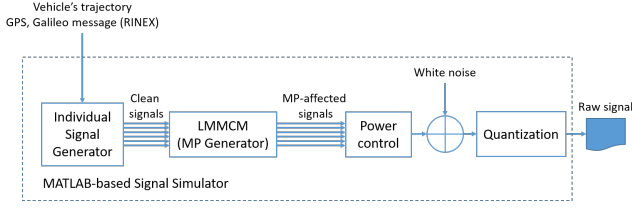
2

Figure 2: Signal simulation scheme

Figure 3: Simulation route

environment on radio signals. The multipath generator can be considered as a filter, using the output of the LMMCM as impulse response.

The process of generating the simulation signal is summarized in Figure 2. Firstly, signals of individual satellites of both GPS and Galileo systems are generated, then passed through the multipath generator to infuse multipath. Afterward, the multipath-affected signals pass through a power control block, which tunes the power of each signal to meet desired C/N_0 setting. All the signals are mixed together, and white noise is added. Then the resulting signal is quantized and saved to output file.

The simulation data was generated with sampling frequency of 16.367 MHz, intermediate frequency of 4.123 MHz, using 5 bits of quantization. The C/N_0 ratio values for all satellites ranges from 37 dB-Hz to 42 dB-Hz, depending on the elevation angles.

The simulation scenario represents a moving vehicle in urban area for 160 seconds with velocity of about 40 km/h. The route is depicted in Figure 3, with a slope of 8% (about 4.6°) from 90 s to 140 s. This slope can be considered typical in urban roads in Vietnam. A short segment of the route is affected by multipath (on all satellites), from 106 s to 154 s. The multipath model was setup in urban surrounding mode, with a road width of 19 m. Both sides of the road were populated with buildings (maximum height 40 m), trees and light posts. To be realistic, in this simulation, the route followed by the car is chosen on the map of Hanoi, Vietnam, and the parameters selected for the multipath model are consistent with the real environment. There are 8 GPS and 6 Galileo satellites visible. The skyplot at the beginning of the simulation is reported in Figure 4.

All the results in this Section are obtained with smoothed pseudoranges.

3.2. Confirmation of measurement error model

To enforce the choice of measurement error model as described in previous section, the model was compared with pseudorange error of the data set being used. On the other hand, at each epoch, a value of C/N_0 ratio was estimated for each satellite, using the 2nd estimator presented in [32]. The absolute pseudorange errors are plotted against C/N_0 values in Figure 5, along with the standard deviation (SD) calculated using the chosen noise model in (3), using *Lightly degraded* setting. It can be observed that the SD line bounds about 51.35% of the points, while the $3\times$ SD line covers about 92.14% of the error. The SD lines for the *Heavily degraded* setting are also plotted here, covering more than 99% of the error for both lines. Since
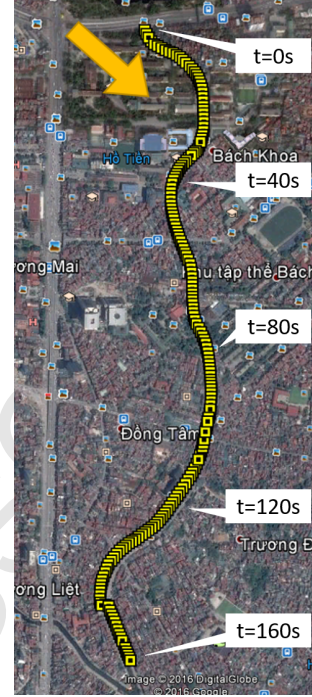
this is excessive and the *Lightly degraded* setting is sufficient to cover the error, the *Lightly degraded* parameter set is chosen for the following experiments.

3.3. Protection Levels

The final step of the algorithm is the PL calculation. In this experiment, the integrity budget is allocated as in Table 2. The integrity budget (or integrity risk) is defined as the probability that the actual positioning error exceed the evaluated PL [2, 4, 25]. Note that the allocation for horizontal direction is much higher than vertical direction, because this algorithm aims at providing integrity assessment for urban environment, which relies more on horizontal direction. The Horizontal Protection Level (HPL) and Horizontal Positioning Error (HPE) for the conventional LS-based ARAIM [5], the Weighted LS residual (WLSR) RAIM [33] and the proposed KF-based ARAIM method are shown in Figure 6 and 7, respectively. On both figures, the highlighted period corresponds to the multipath-affected period.

Figure 6 reports the results for the conventional LS-based ARAIM and the WLSR RAIM. For the whole duration, the HPL of the LS-based ARAIM is about 6 m, even during the multipath period. This is because the noise model of the LS-ARAIM algorithm estimates the noise based on the elevation angles of the satellites, which do not change much during a 160-second period. As a result, the HPL fails to notice the presence of multipath. Meanwhile, the noise model of the WLSR RAIM follows similar approach basing on the satellites' elevation angles, but more inflated to take into account the multipath effect of the urban context. As a result, the HPL of WLSR RAIM is higher - about 26 m to 30 m, quite smooth, and does
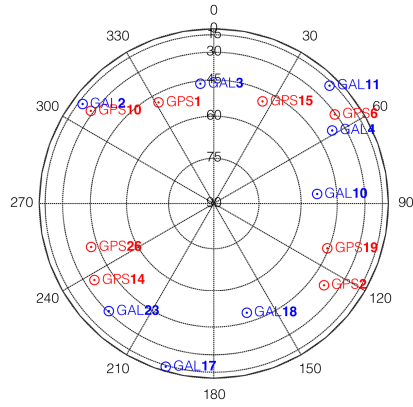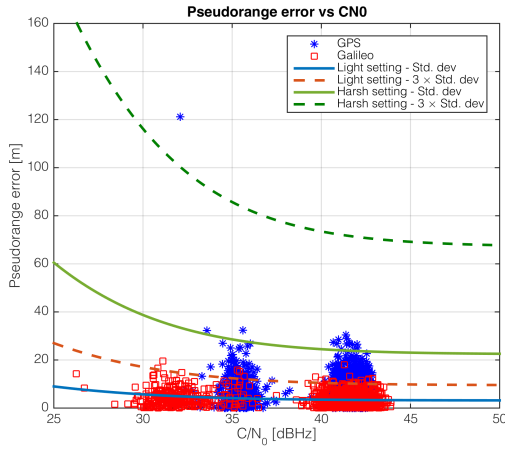
3

Figure 4: Simulation skyplot

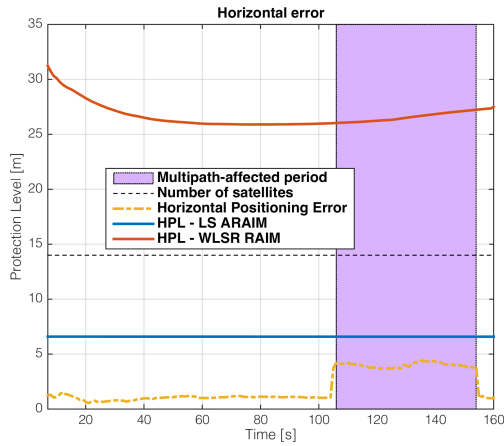Figure 5: Absolute pseudorange errors and SD lines of error models

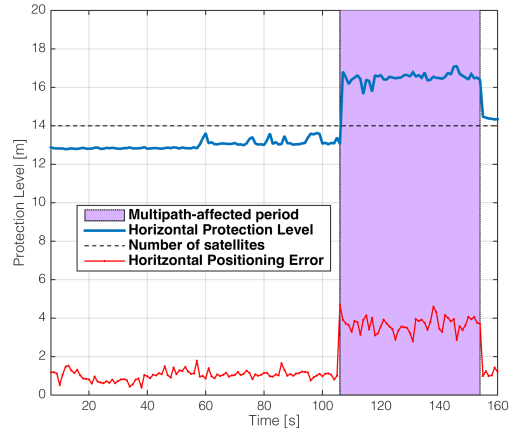Figure 6: HPL and HPE for LS-based ARAIM and WLSR RAIM

Figure 7: HPL and HPE for KF-based ARAIM

Parameters	Values
P_{HMI}	1×10^{-6}
$P_{HMI,HOR}$	9.8×10^{-7}
$P_{HMI,VERT}$	2×10^{-8}

Table 2: Integrity budget allocation

not response to the presence of multipath near the end of the simulation.

215　On the other hand, the KF-ARAIM method's results are shown in Figure 7. During the clean period, the HPL is around 13 m. During the multipath period, as analytically explained in Section 2.1, the multipath decreases the estimated C/N_0, and as a result increases the HPL up to about 17 m. More impor-
220　tantly, the HPL value does follow the change of measurement quality throughout the simulation duration, unlike the LS-based ARAIM's and WLSR RAIM's HPL.

3.4. Performance on real data collection

　Besides the simulation data, the performance analysis has
225　been performed also with real data sets collected in the streets
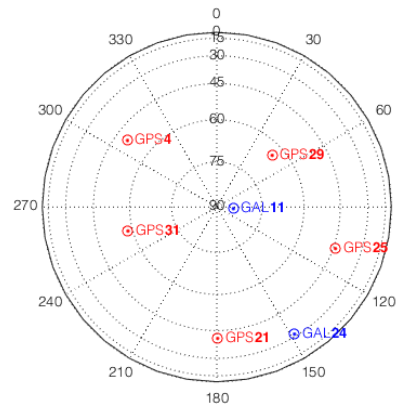

Figure 8: Skyplot of the real data set

of Turin, Italy on a car. The GNSS signals are collected using an ANTCOM antenna, mounted on the roof of the car, connected to the NSL STEREO Frontend [34] and saved to file using a grabber running on a laptop. The reference track was[280] acquired simultaneously by a NovAtel receiver with an Inertial Measurement Unit (IMU) [35], using the same signals splitting from the mounted antenna. The collection is about 800 seconds long. The beginning of the route is a test run in a large courtyard with low building nearby. For the remaining duration, the[285] car moved along normal streets with trees and building on both sides of the road. The data set consists of 5 GPS satellites and 2 Galileo satellites throughout the period. The skyplot of the data set is shown in Figure 8.

The real data set was processed using the proposed KF-based ARAIM algorithm. The positioning results are plotted in Figure 9 as yellow squares. Several segments of interest are[290] also highlighted. The route starts with a test run in a large courtyard with low building nearby - marked as segment A. Segment B sees the car run in a 6-lane street with trees and apartment buildings on both sides of the street. The car stops at segment C for about 100 seconds, due to traffic light. For the remaining segment D, the car continues to move along the 6-lane street.

The HPL for the whole period is depicted in Figure 10, also[295] highlighting the corresponding zones of interest. In general, the HPL provided by the proposed method clearly follows the change of surroundings. The HPL of segment A is about 25-26m and very smooth due to open sky. Segment B sees a higher[300] and less stable PL because of high apartment buildings on both sides of the road. The PL in Segment C is low again, thanks to the car in static position and a park on the right side of the road. Lastly, segment D shows similar effect as Segment B, also[305] due to tall buildings and trees. The number of satellites is also maintained throughout the duration.

On the other hand, the HPL evaluated using the conventional LS ARAIM (in original aviation setting) does not show[310] any variation in correlation with the environment, as in the simulated case. Notably, the LS ARAIM algorithm falsely excluded some satellites at the beginning and the end of the experiment. This is absolutely undesirable considering the already[315] low number of satellites.

4. Discussion

The noise model of the conventional ARAIM algorithm is one of the most important point when adapting the algorithm for different environments. The noise model assumed in the algorithm should reflect the quality of the navigation signals. As-[325] sumption too different from reality may lead to undesired loss of availability, as shown in [24]. The result of the LS ARAIM on real data in section 3.4 further confirms this, as several satellites were excluded from an already limited satellite set. In con-[330] trast, using a C/N_0-based noise model allows the proposed algorithm to follow the change of input quality more closely, thus maintaining availability, in both simulated and real data cases.[335]

5. Conclusion

This paper proposed a KF-based ARAIM algorithm for integrity monitoring method for urban environment. The method was tested on simulation data, which simulates the multipath effect often encountered in urban scenario, as well as real data collected in urban area of Turin, Italy. The results in both cases validate the method, since the PL follows the change of measurement quality as the vehicle passes through different areas, while maintaining integrity and availability. Comparative results with LS-based ARAIM further confirms the suitability of the proposed method for urban scenario.

Acknowledgment

References

[1] U. DoD, U. DHS, U. DoT, Federal radionavigation plan, Tech. rep., DOT-TSC-RSPA-84.8 (2012).

[2] E. D. Kaplan, C. J. Hegarty, Understanding GPS: principles and applications, Artech House: Norwood, MA, USA, 2005.

[3] S. Andrés, C. Daniel, Integrity monitoring applied to the reception of gnss signals in urban environments, Ph.D. thesis (2012).

[4] B. W. Parkinson and J. J. Spilker, Chapter 5: Receiver Autonomous Integrity Monitoring Global Positioning System: Theory and Applications, American Institute of Aeronautics and Astronautics, USA, 1996.

[5] Working Group C - ARAIM Technical Subgroup, Interim Report.

[6] FAA GEAS Panel, Phase II of the GNSS evolutionary architecture study, Report. GNSS Evolutionary Architecture Study Panel.

[7] J. Blanch, T. Walter, P. Enge, S. Wallner, F. Amarillo Fernandez, R. Dellago, R. Ioannides, I. Fernandez Hernandez, B. Belabbas, A. Spletter, M. Rippl, Critical elements for a multi-constellation advanced raim, Navigation 60 (1) (2013) 53–69. doi:10.1002/navi.29.
URL http://dx.doi.org/10.1002/navi.29

[8] J. Blanch, A. Ene, T. Walter, P. Enge, An Optimized Multiple Hypothesis RAIM Algorithm for Vertical Guidance, in: Proceedings of the 20th International Technical Meeting of the Satellite Division of The Institute of Navigation (ION GNSS 2007), 2007.

[9] J. Blanch, T. Walter, P. Enge, Y. Lee, B. Pervan, A. Spletter, Advanced raim user algorithm description: Integrity support message, in: Proceedings of the 25th International Technical Meeting of The Satellite Division of the Institute of Navigation (ION GNSS 2012), 2012, pp. 2828–2849.

[10] H. T. Tran, L. Lo Presti, Demonstration of Multi-GNSS Advanced RAIM Algorithm Using GPS and Galileo Signals, ICSANE 2013 (International Conference on Space, Aeronautical and Navigational Electronics 113 (335) (2013) 191–196.

[11] A. El-Mowafy, B. S. Arora, The Current ARAIM Availability According to LPV-200 Using GPS and BeiDou in Western Australia, in: IGNSS2013 Symposium - The International Global Navigation Systems Society (IGNSS), 2013, pp. 1–16.

[12] H. Mei, X. Zhan, X. Zhang, Gnss vulnerability assessment method based on araim user algorithm, in: 2017 Forum on Cooperative Positioning and Service (CPGPS, 2017, pp. 111–115. doi:10.1109/CPGPS.2017.8075107.

[13] J. Cosmen-Schortmann, M. Azaola-Saenz, M. A. Martinez-Olague, M. Toledo-Lopez, Integrity in urban and road environments and its use in liability critical applications, in: 2008 IEEE/ION Position, Location and Navigation Symposium, 2008, pp. 972–983. doi:10.1109/PLANS.2008.4570071.
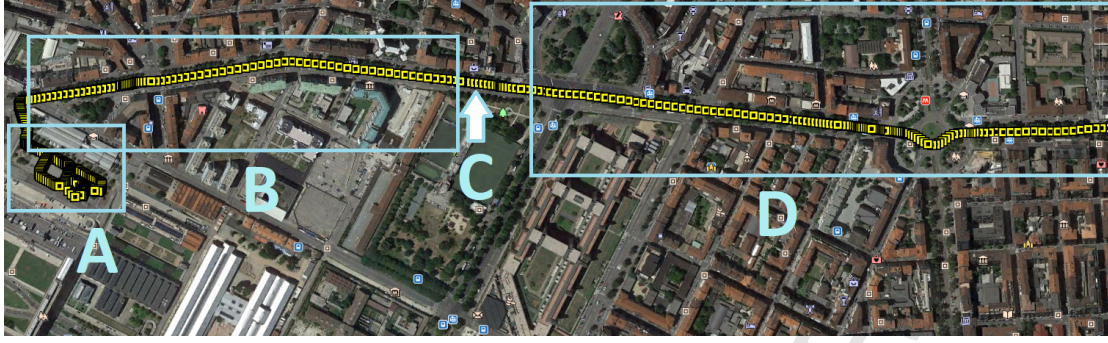
5

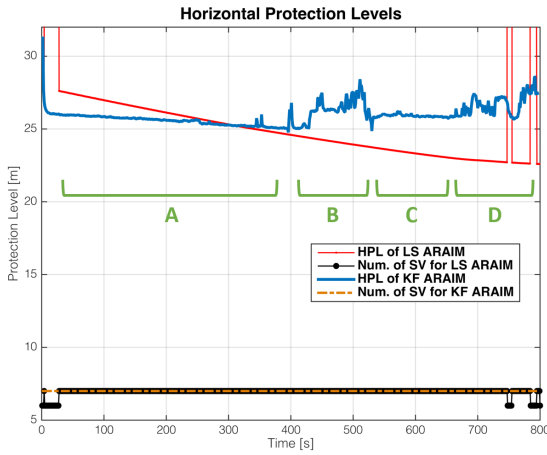Figure 9: Positioning results of the real data collection

Figure 10: HPL of the real data collection evaluated by KF-based ARAIM and LS-based ARAIM

[14] R. Toledo-Moreo, D. Betaille, F. Peyret, Lane-level integrity provision for navigation and map matching with gnss, dead reckoning, and enhanced maps, IEEE Transactions on Intelligent Transportation Systems 11 (1) (2010) 100–112. doi:10.1109/TITS.2009.2031625.

[15] P. D. Groves, Z. Jiang, M. Rudi, P. Strode, A portfolio approach to nlos and multipath mitigation in dense urban areas, in: Proceedings of the 26th International Technical Meeting of The Satellite Division of the Institute of Navigation (ION GNSS+ 2013), The Institute of Navigation, 2013, pp. 3231 – 3247.

[16] P. Xie, M. G. Petovello, Measuring gnss multipath distributions in urban canyon environments, IEEE Transactions on Instrumentation and Measurement 64 (2) (2015) 366–377.

[17] Z. Jiang, P. D. Groves, W. Y. Ochieng, S. Feng, C. D. Milner, P. G. Mattos, Multi-constellation gnss multipath mitigation using consistency checking, in: Proceedings of the 24th International Technical Meeting of The Satellite Division of the Institute of Navigation (ION GNSS 2011), The Institute of Navigation, 2011, pp. 3889–3902.

[18] J. Santa, B. Ubeda, R. Toledo, A. F. G. Skarmeta, Monitoring the position integrity in road transport localization based services, in: IEEE Vehicular Technology Conference, 2006, pp. 1–5. doi:10.1109/VTCF.2006.575.

[19] R. Toledo-Moreo, J. Santa, M. A. Zamora-Izquierdo, B. Ubeda, A. F. Gómez-Skarmeta, A study of integrity indicators in outdoor navigation systems for modern road vehicle applications, in: 2nd Workshop on Planning, Perception and Navigation for Intelligent Vehicles, IEEE/RSJ 2008 International Conference on Intelligent Robots and Systems. Nice, France, 2008.

[20] T. Binjammaz, A. Al-Bayatti, A. Al-Hargan, Gps integrity monitoring for an intelligent transport system, in: 2013 10th Workshop on Positioning, Navigation and Communication (WPNC), 2013, pp. 1–6. doi:10.1109/WPNC.2013.6533268.

[21] O. Le Marchand, P. Bonnifait, J. Bañez-Guzmán, F. Peyret, D. Betaille, Performance Evaluation of Fault Detection Algorithms as Applied to Automotive Localisation, in: European Navigation Conference - GNSS 2008, Toulouse, France, 2008.
URL https://hal.archives-ouvertes.fr/hal-00445170

[22] G. Gargiulo, M. Leonardi, M. Zanzi, G. Varacalli, Gnss integrity and protection level computation for vehicular applications, in: Proceedings of the 16th Ka and Broadband Communications Navigation and Earth Observation Conference, Vol. 2022, Milan, Italy, 2010.

[23] L. Zhang, J. Li, T. Cui, S. Liu, An adapted raim algorithm for urban canyon environment, in: 2017 Forum on Cooperative Positioning and Service (CPGPS, 2017, pp. 116–121. doi:10.1109/CPGPS.2017.8075108.

[24] H. T. Tran, T. T. Hai, L. Lo Presti, Adaptation of ARAIM Algorithm for Urban Environment Applications, in: Proceeding of International Symposium on GNSS 2015, 2015.

[25] H. T. Tran, G. Belforte, An ARAIM Adaptation for Kalman Filter, in: Workshop on Maritime Navigation and Communication (ComNavi 2017), 2017, pp. 27–37, available at http://porto.polito.it/2695825/1/Belforte_129_C_73r.pdf. Last visited January 10, 2017.

[26] R. Inc., Minimum operational performance standards for global positioning system/wide area augmentation system airborne equipment (December 2006).

[27] G. A. McGraw, Development of the LAAS accuracy models, in: Proceedings of the 13th International Technical Meeting of The Satellite Division of The Institute of Navigation (ION GPS 2000), 2000, pp. 1212–1223.

[28] H. Kuusniemi, User-Level Reliability and Quality Monitoring in Satellite-Based Personal Navigation, Tampere University of Technology, 2005.

[29] T. L. L. Thuan, N.D.; Tung, A software based multi-IF output simulator, in: Proceedings of the International Symposium of GNSS (IS-GNSS), 2015.

[30] A. Lehner, A. Steingass, A novel channel model for land mobile satellite navigation, in: Institute of Navigation Conference ION GNSS, 2005, pp. 13–16.

[31] ITU, Propagation data required for the design of earth-space land mobile telecommunication systems (2009).

[32] N. C. Beaulieu, A. S. Toms, D. R. Pauluzzi, Comparison of four snr estimators for qpsk modulations, IEEE Communications Letters 4 (2) (2000) 43–45. doi:10.1109/4234.824751.

[33] C. D. S. Andres, Integrity monitoring applied to the reception of gnss signals in urban environments (July 2012).

[34] NSL: Software Defined Radio GNSS Solutions, Available at http://www.nsl.eu.com/primo.html, last visited November 21, 2017.

[35] SPAN-CPT Single Enclosure GNSS/INS Receiver, Available at https://www.novatel.com/products/span-gnss-inertial-systems/span-combined-systems/span-cpt/, last visited November 21, 2017.